Acta Materialia Transylvanica 8/2. (2025) 96–104.
DOI: Hungarian: https://doi.org/10.33923/amt-2025-02-09
English: https://doi.org/10.33924/amt-2025-02-09

Compression Strength Testing of Grey Poplar

Fanni SZŐKE,[1] Sándor TÁRKÁNYI,[2] Antal KÁNNÁR[3]

[1] *University of Sopron, Faculty of Wood Engineering and Creative Industries, Institute of Creative Industries, Sopron, Hungary, Szoke.Fanni@phd.uni-sopron.hu*

[2] *University of Sopron, Faculty of Wood Engineering and Creative Industries, Institute of Creative Industries, Sopron, Hungary, tarkanyi.sandor@uni-sopron.hu*

[3] *University of Sopron, Faculty of Wood Engineering and Creative Industries, Institute of Creative Industries, Sopron, Hungary, kannar.antal @uni-sopron.hu*

Abstract

Knowledge of the strength values of Populus canescens is important for expanding the range of applications of this species. The use of wood as an orthogonally anisotropic material in structural engineering is significantly influenced by its strengths in different anatomical directions. The results obtained from tensile and compressive strength tests of test specimens in the main anatomical directions allow the determination of the strength surface, which makes it possible to determine the strength of wood in any direction. A further within-group classification is provided by the separation of sapwood and duramen, so that the strength behaviour of the individual wood sections within the wood body can be revealed in addition to the different ultimate strengths.

Keywords: *grey poplar, strength surface, anisotropy.*

1. Introduction

Research in forestry has shown that increasing average annual temperatures and decreasing precipitation has led to increased mortality of sensitive tree species [1]. Poplar (Populus canescens), which is indigenous to Hungary and has a significant native population, offers an excellent opportunity to replace declining populations due to climate change. It is a fast-growing, highly productive species, occupying 1.5 million hectares of forest area in today's Hungarian forestry, of which 1.3-1.5 million m3 of timber is traded annually. This volume represents 23-25% of the total annual timber production. Its use is to produce crates, pallets, coasters, particleboard, fibreboard [2]. Its structural use is in principle possible due to its higher-than-average density of poplar species, but further strength testing is needed for predictable design. The present research aims to determine the strength surfaces resulting from anisotropic properties in different anatomical shapes.

2. Materials and methods

The sapwood and the heartwood parts of the grey summer are clearly separated. The moisture content of the strap, present in a proportion of 30-40%, is higher than that of the gizzard, but the literature shows that there is no significant difference in their physiological characteristics. In the design of the test specimens, the separation of the two parts of the wood was taken into account to obtain more distinct strengths for each part and to avoid results that are influenced by the different moisture content. Care must be taken to ensure that the specimens are of the correct length dimensions. If the specimen is too long, the normal stresses from compression will be accompanied by buckling and stress from bending, while if the specimen is too short, the stress plateau at the transfer locations will influence the linear stress-strain state of the central part. The ideal size is defined in the literature as a length of the test specimen 2-3 times the minimum cross-sectional dimension [3, 4]. On this basis, I have defined the nominal size of my own specimens as 20 × 20 × 50

mm. In the strength tests, the consideration of anatomical directions on the specimens was given priority. As shown in the first figure, longitudinal (L), radial (R), tangential (T) directions and their planes were distinguished, on which specimens with 0°, 45° and 90° designs were prepared depending on the direction (Fig. 1). The multi-directional specimens made it possible to determine the strength surfaces later.

The 45° fibre run is used to experimentally determine the shear strength, based on Askenazi's anisotropic strength theory and practical experience [3]. The design allows the specimens to shear parallel to the principal axis of the anatomical principal planes, despite normal loading, with normal and shear stresses. Pure shear will still not occur, but the distribution of shear stress along the shear cross section will be uniform, which is not the case with other methods. The influence of normal stresses on the shear stress can be determined by a comparison between the maximum of the principal stress functions of the tensile and compressive strength tests, which are shown to have no influence on the shear strength within a certain probability level. Thus, shear strength can be indirectly determined by tensile strength measurements [4].

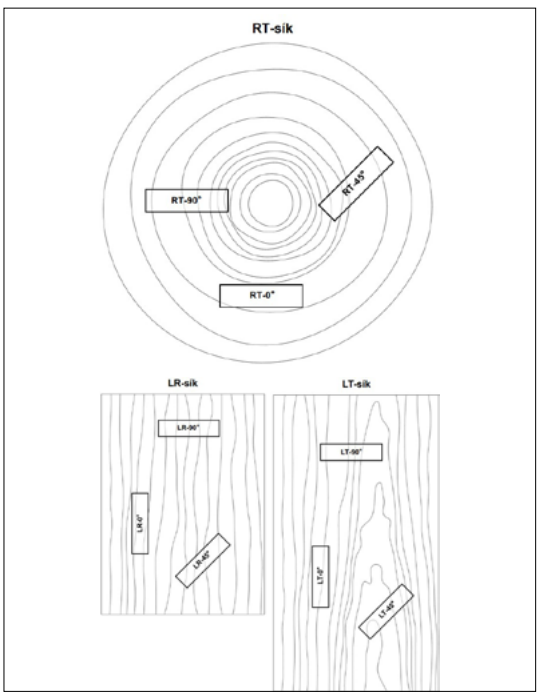

Fig. 1. *Directional design of the test specimens.*

Thus, shear strength can be indirectly determined by tensile strength measurements. During the tests, 30 straps and the same number of studs per direction - LR0°, LR45°, LR90°, LT45°, LT90°, RT45° - were measured for compressive strength in a total of about 400 test specimens, using an Instron 5985 universal material testing machine. With this number of specimens, strength values can be determined with an accuracy of about 0.2 MPa. The measurement procedure was based on the ISO 13061-17 standard, which specifies, among other things, that the tests should be conducted for a period of between 1 and 5 minutes until the specimen breaks. [5] In order to achieve the standard, the instrument test speed was calibrated to 0.6 mm/min, but due to the anatomical orientation and different strengths of the LT90 and LR45 gauge specimens, the speed had to be increased to 1.2 mm/min for the LT90 and LR45 heartwood specimens and 1.8 mm/min for the LR45 sapwood and LT45 specimens. Moisture content was determined by wet and absolute dry mass, converted to 12% air dry mass using the standard conversion formula (1). The compressive strength is represented by „σ", „u" is the moisture content, „α" is a correction factor for the variation of the Si-strength per moisture content, with a value of 0.04 [5]:

$$\sigma_{12} = \sigma_U[1 + \alpha(U - 12)] \quad (1)$$

The stress values thus corrected, calculated as the ratio of the maximum force to the head area, can be considered for the literature comparison, which also refer to air-dry strength.

In addition, the elastic modulus of the test specimens has been determined, which also influences the shape of the curves presented later. To do this, the specific length change must be expressed as the ratio of the total length change to the original length (2):

$$\varepsilon = \frac{\Delta L}{L} \quad (2)$$

The modulus of elasticity can be defined as the ratio of the compressive stress divided by the corresponding specific strain in the linear elastic range, given the data (3):

$$E = \frac{\sigma}{\varepsilon} \quad (3)$$

The calculations were performed on the results of all samples to exclude measurement errors and then evaluated, considering the minimum, maximum, mean, standard deviation.

3. Results and their evaluation

During the test, the instrument produced a force-displacement diagram for each specimen, which clearly shows the failure and its extent. The individual sections can be clearly identified in each case. The first stage was surface levelling, followed by a linear rising stage, which showed a steady absorption of the force. Its steepness was influenced by the elastic modulus. In the third phase, cracks in the specimen were not visible until the point of maximum force absorption. Fracture of the wood structure, with visible stump loss, occurred in the fourth and final phase, which the instrument continued until a 40% setback. All tests were performed up to the point of visual failure.

The force-displacement diagrams of the LR0 sapwood specimens show the different phases (Fig. 2). The linear phase is followed by a curved phase, the failure is observed in the fourth and final phase, where there is no sudden breakage, only a slight decrease in force. The strength data are shown in Table 1–6.

In the same direction, the test specimens in the heartwood showed a slightly lower force absorption (Fig. 3), while a much more significant decrease was observed in the failure section. The sudden jump was caused by specimen fracture.

According to the literature, several different basic types of fracture patterns can be distinguished in the longitudinal direction parallel to the fibres, such as collapse, wedge-shaped cleavage, shearing, splitting, collapse and splitting, and end sliding and opening [6]. The fracture pattern typical of these specimens during testing is shown in the following figure (Fig. 4). It can be clearly seen that the most typical failure mode is shearing, which is associated with small cracks in the heartwood specimen, which is the cause of the failure mode shown in the diagram.

In the LR45 direction, the typical diagrams of the sapwood patterns (Fig. 5) start with a steep linear phase, followed in all cases by an abrupt change to a steeper phase with a smaller slope in the third, unobservable failure stage. In the fourth stage, after continuous fragmentation, there was a sudden stump transition.

The heartwood specimens produced a curve with a smaller slope than the sapwood, without any prominent change (Fig. 6). After the gradual cracking in the stub-retraction section, a sudden fracture occurred, causing the specimen to separate.

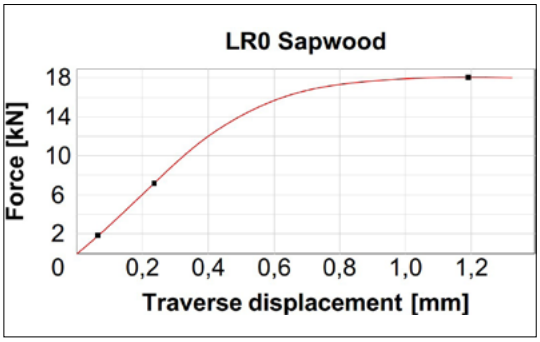

Fig. 2. *Force-displacement diagram – LR0 sapwood.*

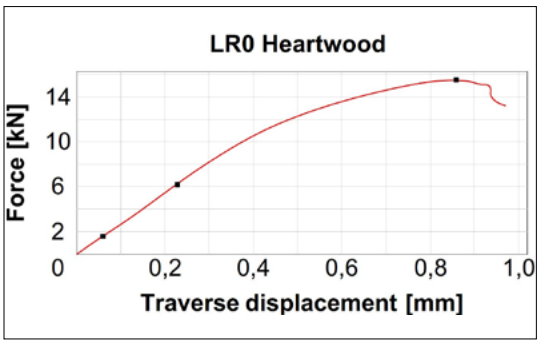

Fig. 3. *Force-displacement diagram – LR0 heartwood*

Fig. 4. *Typical fracture pattern of the test specimens – LR0.*

The fracture patterns (Fig. 7) typically showed collapse and shear along the annual rings in the case of the sapwood. The specimens remained intact with significant residual deformation. In all cases, the heartwood was brittle, and the fracture patterns were characterised by shearing, resulting in separation of the test specimen without significant permanent deformation.

The diagram of the LR90 sapwood specimens (Fig. 8) shows a steady slope, with no abrupt

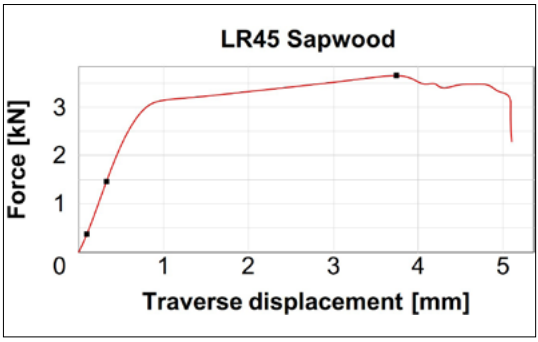

Fig. 5. *Force-displacement diagram – LR45 sapwood.*

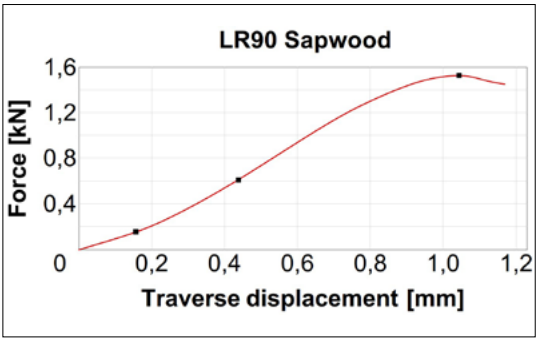

Fig. 8. *Force-displacement diagram – LR90 sapwood.*

Fig. 6. *Force-displacement diagram – LR45 heartwood.*

Fig. 9. *Force-displacement diagram – LR90 heartwood.*

Fig. 7. *Typical fracture pattern of the test specimens – LR45*

Fig. 10. *Typical fracture pattern of the test specimens – LR90.*

breakage even at the failure stage. The fibres compressed gradually and proportionally during the test.

The heartwood (**9. ábra**) shows a similar curve, except for the last section, where in almost all cases there was a significant drop after the point of maximum force application, indicating a sudden crack. This process was so rapid that the test specimen started to regain strength, which was observed on the minor uphill section.

According to the literature, tangential and radial stress-indicating fractures in the perpendicular to the rostra are the collapse of an area of the early pastes (shearing along a tree-ring) and the bulging of tree-rings **[6]**.] In the case of the sapwood, the early lattice was characterised by collapse, while the heartwood was also characterised by shearing, which was also reflected in the protrusion of the growth ring (**Fig. 10**).

The diagram of the LT45 sapwood specimen (Fig. 11) shows the same pattern as the LR45 sapwood, however, in the failure phase there were no sudden shift-zones, a low intensity decreasing phase was observed.

The heartwood samples also showed a similar curve with a smaller slope in the linear phase (Fig. 12). AThe rapid decrease in the scale in the last phase was caused by the complete fracture of the specimen.

The fracture patterns for the LT45 specimens (Fig. 13) were characterised by shear, associated with a kind of „S" shaped permanent deformation of the sapwood, with the tensile sides splitting. In the case of a heartwood, the specimens separated without significant deformation.

In the case of LT90 (Fig. 14) a relatively abrupt linear section occurred, but at the same time the visible failure did not occur in the form of a fracture, as can be seen in the diagram.

In contrast, the LT90 heartwood specimens showed a non-significant but more easily distinguishable loss of integrity on the curve (Fig. 15).

The typical fracture pattern of the LT90 specimens (Fig. 16) can be compared with the literature described for the LR90 specimens. In a

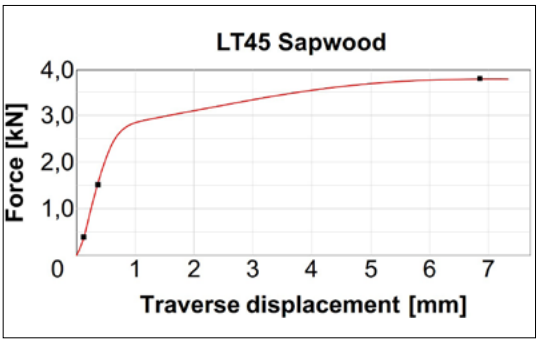

Fig. 11. *Force-displacement diagram – LT45 sapwood.*

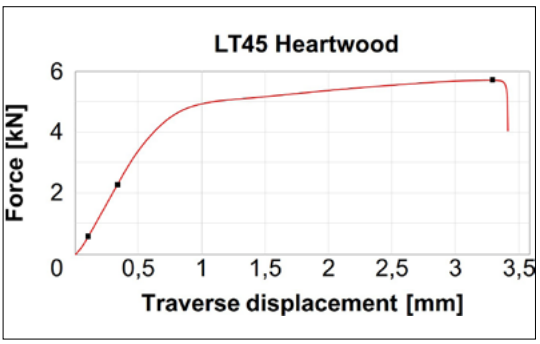

Fig. 12. *Force-displacement diagram–LT45 heartwood.*

Fig. 13. *Typical fracture pattern of the test specimens – LT45.*

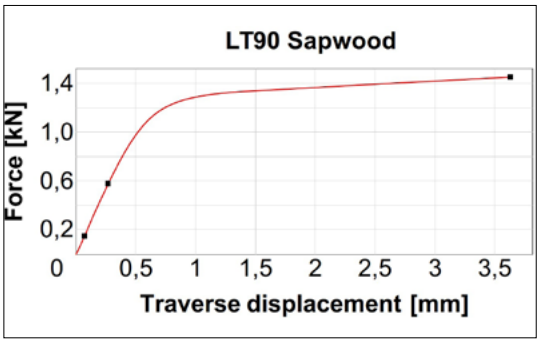

Fig. 14. *Eorce-displacement diagram – LT90 sapwood.*

Fig. 15. *Force-displacement diagram – LT90 heartwood.*

Fig. 16. *Typical fracture pattern of the test specimens – LT90.*

tangential direction, it is characterised by the protrusion of the annual rings, both in the case of the sapwood and the heartwood. Both specimen types suffered permanent deformation, which was more significant in the case of heartwood.

The RT45 sapwood specimens (Fig. 17) showed a slight decrease in the failure rate after the point of maximum force application, with no sudden fracture pattern.

The heartwood curve followed a similar pattern (Fig. 18), but in the last stage a decreasing as-case indicating a gradual destruction appeared. The small jumps indicated the breakage of the tree rings.

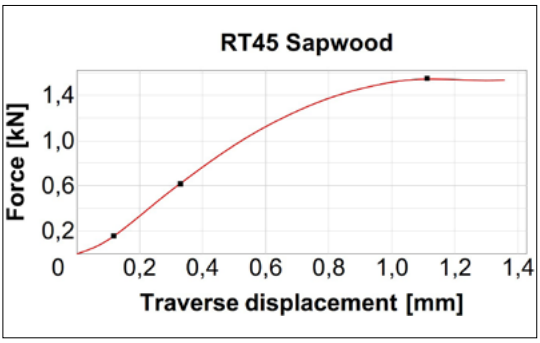

Fig. 17. *Force-displacement diagram – RT45 sapwood.*

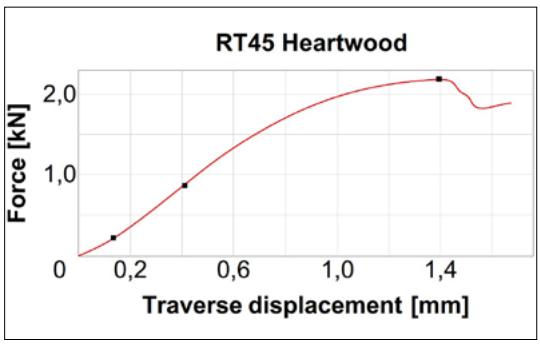

Fig. 18. *Force-displacement diagram – RT45 heartwood.*

Fig. 19. *Typical fracture pattern of the test specimens – RT45.*

A typical failure pattern in the tangential and radial directions is the buckling of the annual rings (Fig. 19). The fracture pattern in the sapwood was almost all annual rings, in the heartwood the whole specimen showed permanent buckling.

The slope of the linear section of the diagrams is determined by the elastic modulus in the linear elastic range, which can be determined from the formulas presented earlier. The following figures show the values of the elastic modulus in each direction, separately for the sapwood and the heartwood, as a function of the width of each specimen. The exact average values are presented in tabular form.

For the LR0 specimens (Fig. 20) all parts showed similar elasticity values, the heartwood having a minimally higher average, but also a higher dispersion than the sapwood, due to the more brittle behaviour.

The LR45 specimens showed much larger differences (Fig. 21). While the sapwood fitted tightly to a value, the heartwood showed not only a large variance, but also much larger results, not only on average but also considering its minimum values.

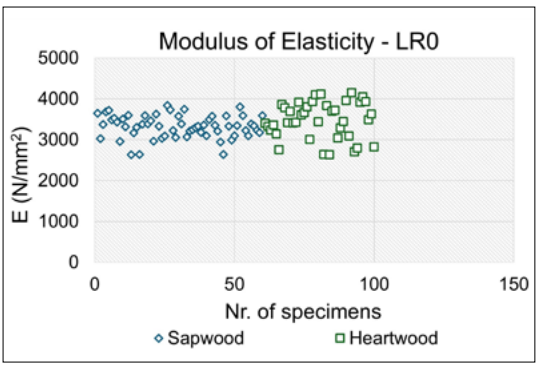

Fig. 20. *Modulus of elasticity values - LR0.*

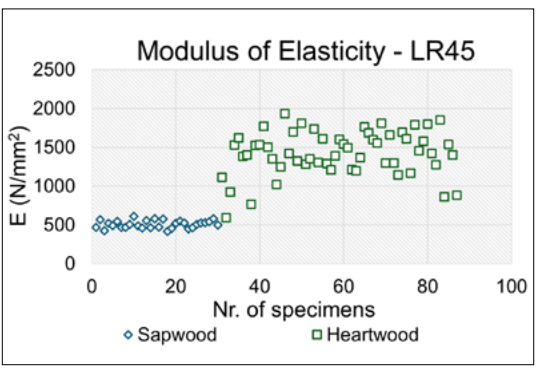

Fig. 21. *Modulus of elasticity values – LR45.*

The elastic modulus values of the LR90 specimens also show a difference between the sapwood and the heartwood (Fig. 22). This variance is significant in all cases but is also easily distinguishable relative to each other. The heartwood gave a higher average value.

The results for the LT45 specimens (Fig. 23) were distinct in terms of elastic modulus values, however, the average of the heartwood was only slightly higher than the average of the sapwood. The scatter of the heartwood was larger, with minimum values below the minimum of the sapwood. Compared to the LR45 specimens, the sapwood showed a higher scatter, but the difference between the two logs was less.

LIn the LT90 direction, the dispersion of the sapwood and heartwood values was almost equal, with the average of the sapwood values below the average of the heartwood values (Fig. 24).

The elastic modulus values of the RT45 specimens were also divided into mixed groups of sapwood and heartwood (Fig. 25). The experiment included specimens that included the sapwood - heartwood boundary along the entire length and hence the properties of both parts were characterized. The variation was large for each group, with the averages being larger for heartwood. The mixed samples represented a kind of average between the two parts.

Based on the results presented, the following tables show the averages, minimum, maximum, standard deviation, and percentage of standard deviation values for compressive strength, elastic modulus, the lower the smaller the value, the more dependable the material behaviour. The fc.k refers to the quantiles in the lower 5%, which are used to determine the strength class. The comparison is based on the strength values of the Eurocode5 series of standards, also used in structural design, which also consider the lower 5% quantile of the characteristic value [7]. 45° specimens are not covered by the standard and cannot be classified (N.C.). LR0 is for the pressure parallel to the fibre, LR90 and LT90 are for the pressure perpendicular to the fibre.

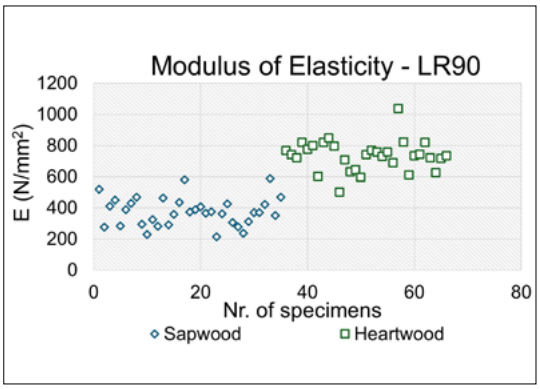

Fig. 22. *Modulus of elasticity values – LR90.*

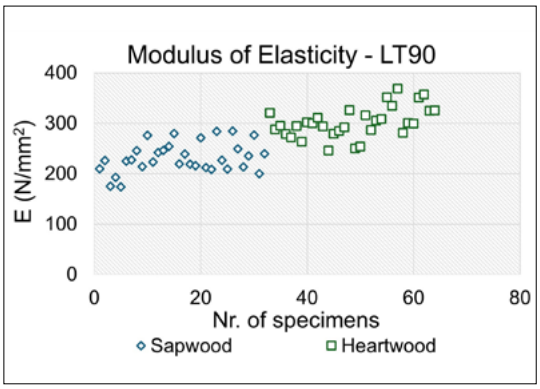

Fig. 24. *Modulus of elasticity values – LT90.*

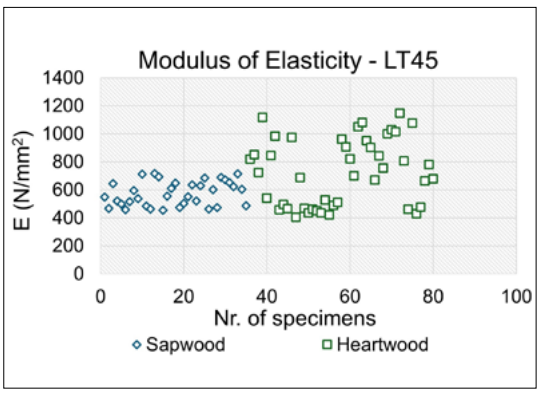

Fig. 23. *Modulus of elasticity values – LT45.*

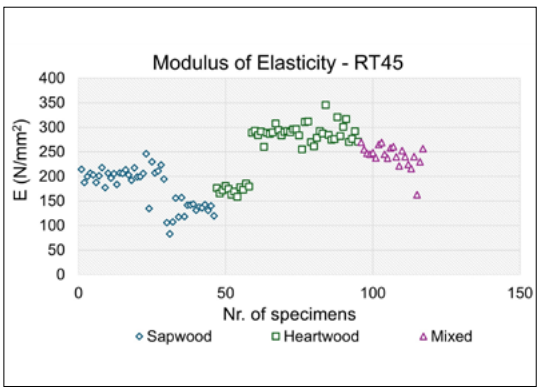

Fig. 25. *Modulus of elasticity values – RT45.*

Table1. *LR0 – pressure parallel to the fibre*

LR0 – pressure parallel to the fibre (N/mm²)			
Sapwood		Heartwood	
Average	33.72	Average	33.02
Min.	24.71	Min.	21.48
Max.	38.18	Max.	41.01
Std. dev.	2.85	Std. dev.	5.17
Std. d. %	8.46	Std. d. %	15.66
Sapwood and heartwood together			
σ_{12}	33.44	$f_{c.k}$	24.93
E_{mean}	3384	Szil. o.	C30

Table 2. *LR45 – 45° pressure to the fibre*

LR45 – 45° pressure to the fibre (N/mm²)			
Sapwood		Heartwood	
Average	7.26	Average	11.48
Min.	5.69	Min.	5.04
Max.	8.62	Max.	16.44
Std. dev.	0.64	Std. dev.	2.69
Std. d. %	8.88	Std. d. %	23.45
Sapwood and heartwood together			
σ_{12}	10.02	$f_{c.k}$	5.74
E_{mean}	1108.5	Szil. o.	N. B.

Table 3. *LR90 – pressure perpendicular to the fibre*

LR90 – pressure perpendicular to the fibre (N/mm²)			
Sapwood		Heartwood	
Average	3.74	Average	5.93
Min.	2.87	Min.	4.48
Max.	4.53	Max.	8.83
Std. dev.	0.50	Std. dev.	0.91
Std. d. %	13.44	Std. d. %	15.32
Sapwood and heartwood together			
σ_{12}	4.77	$f_{c.k}$	3.79
E_{mean}	543.6	Szil. o.	C50

Table 4. *LT45 – 45° pressure to the fibre*

LT45 – 45° pressure to the fibre (N/mm²)			
Sapwood		Heartwood	
Average	8.28	Average	9.19
Min.	6.88	Min.	6.02
Max.	9.43	Max.	14.09
Std. dev.	0.80	Std. dev.	2.80
Std. d. %	9.70	Std. d. %	30.42
Sapwood and heartwood together			
σ_{12}	8.79	$f_{c.k}$	6.50
E_{mean}	661.1	Szil. o.	N. B.

Table 5. *LT90 – pressure perpendicular to the fibre*

LT90 – pressure perpendicular to the fibre (N/mm²)			
Sapwood		Heartwood	
Average	2.62	Average	3.81
Min.	1.78	Min.	2.91
Max.	3.32	Max.	4.69
Std. dev.	0.40	Std. dev.	0.42
Std. d. %	15.20	Std. d. %	10.96
Sapwood and heartwood together			
σ_{12}	3.22	$f_{c.k}$	2.49
E_{mean}	266.7	Szil. o.	C22

Table 6. *RT45 – 45° pressure to the fibre*

RT45 – 45° pressure to the fibre (N/mm²)			
Sapwood		Heartwood	
Average	2.46	Average	3.34
Min.	1.82	Min.	0.77
Max.	3.05	Max.	4.49
Std. dev.	0.41	Std. dev.	0.81
Std. d. %	16.86	Std. d. %	24.18
Mixed		Sz + g + v	
Average	3.27	σ_{12}	2.98
Min.	2.96	E_{mean}	223.6
Max.	3.70	$f_{c.k}$	2.51
Std. dev.	0.21	Szil. o.	N. B.
Std. d. %	6.48		

4. Conclusions

From the above measurement results, it can be concluded that the wood showed significantly different behaviour between the diverse types of wood. This can be seen from the diagrams drawn during the tests, which also indicate the behaviour and the type of deterioration. Significant differences between the sapwood and the heartwood sections were observed during the measurements. The sapwood grid showed more spring-like behaviour, the fibres slid and deformed, but the specimen remained in one piece. When the heartwood was destroyed, much more brittle fracture patterns were observed, mostly with specimens separating, fibres tearing and breaking. The Modulus of elasticity values also showed significantly different behaviour as a function of the sapwood and the heartwood, with scatter values as shown in the tables. The elastic modulus and strength values were also determined for both logs together, considering their working together. To determine the strength values that can be measured in practice, the lower 5% quantiles were calculated and then classified into a strength class. The results showed that the sapwood, despite its lower strength results, showed a more reliable and elastic behaviour with low variance. On the other hand, the heartwood had higher measuring values, but its brittle behaviour gave more unpredictable results with higher scatter.

Based on the results, it can be concluded that the strength of grey poplar reaches the strength requirements of structural timber and can be recommended as a structural material, thus replacing imported pine.

References

[1] Gálos B., Führer E.: *A klíma erdészeti célú előrevetítése.* Erdészettudományi Közlemények, 8/1. (2018) 43–55. https://www.doi.org/10.17164/EK.2018.003

[2] Molnár S., Farkas P.: *Nyár (nyár fajok) – Populus spp*. In: *Földünk ipari fái* (2nd ed.), Eds. Molnár S., Farkas P., Börcsök Z., Zoltán Gy., Photog. Richter H.G., & Szeles P., Faipari Tudományos Egyesület, Sopron, ISBN 978-963-12-5239-2, 97–99.

[3] Askenazi E. K.: *Anizotropia dreveszinü i drevesznüh materialov (A fa- és faalapú anyagok anizotrópiája)*. 1. kiadás. Lesznaja Promüslennoszty, Moszkva, 1978. 97-99.

[4] Szalai J.: *A faanyag és faalapú anyagok anizotróp rugalmasság- és szilárdságtana.* 1. rész. A mechanikai tulajdonságok anizotrópiája. Erdészeti és Faipari Egyetem, Sopron, 1994. 286–293.

[5] EN ISO 13061-17: Physical and Mechanical Properties of Wood – Test Methods for Small Clear Wood Specimens-. Part 17: Determination of Ultimate Stress in Compression Parallel to Grain. 2017.

[6] Bodig J.: *The Effect of Anatomy on the Initial Stress-Strain Relationship.* Forest Products Journal, 15/5. May 1965. 197-202.

[7] Armuth M., Bodnár M.: Fa tartószerkezetek – Tervezés az Eurocode alapján. 3. aktualizált és bővített kiadás. Artifex Kiadó Kft., Budapest, 2018. 19.